Adaptive Coordinated Formation Control of Heterogeneous Vertical Takeoff and Landing UAVs Subject to Parametric Uncertainties

Yao Zou, Haojie Zhang, and Wei He, *Senior Member, IEEE*

***Abstract*—This article focuses on the solution to the coordinated formation problem of heterogeneous vertical takeoff and landing (VTOL) unmanned aerial vehicles (UAVs) in the presence of parametric uncertainties. In particular, their inertial parameters are distinct and unavailable. For the sake of the accomplishment of the coordinated formation objective of multiple underactuated VTOL UAVs through local information exchange, an adaptive distributed control algorithm is developed under a cascaded structure. Specifically, by introducing an immersion and invariance (I&I) adaption strategy for the exponential mass estimation, a distributed command force is first synthesized in the position loop. Next, an applied torque with adaption is synthesized for the attitude tracking to a command attitude. This command attitude, as well as the applied thrust, is extracted from the synthesized command force without singularity. It is shown in terms of the Lyapunov theory that driven by the proposed adaptive distributed control algorithm, the concerned coordinated formation control of multiple VTOL UAVs is achieved asymptotically. Finally, an illustrative example is simulated to validate the effectiveness of the proposed control algorithm.**

***Index Terms*—Adaption, distributed control, formation control, immersion and invariance (I&I), unmanned aerial vehicles (UAVs).**

I. INTRODUCTION

ALONG with the rapid development of disciplines on artificial intelligence, informatics, electronics, mechanics, etc. [1]–[3], considerable concern has been paid to the autonomous operation of unmanned aerial vehicles (UAVs). As a typical representative, vertical takeoff and landing (VTOL) UAVs have been extensively applied in military and civil fields due to their characteristics in hovering, low-speed or low-altitude flight, and agile motion [4]. On the other hand, to accomplish some intricate missions efficiently without costly expenses, the coordinated formation of multiple micro VTOL UAVs, rather than a single monolithic one, is feasible in practice [5]. However, affected by internal parametric uncertainties and external interaction manners, there are still challenges in developing coordinated control algorithms.

Since a typical VTOL UAV system is underactuated in nature, a majority of its control approaches are based on a cascaded structure of a two-level architecture [6]. In terms of such a cascaded structure, the "high-level" outer position and "low-level" inner attitude loop can be surveyed sequentially [4]. Inspired by this idea, a number of control methods have been proposed for the tracking of a single VTOL UAV (see [7]–[11] and references therein). However, frustrated by parametric uncertainties, in practice, it is inevitable that the tracking performance will be adversely affected. Even worse, a severe parameter deviation may destroy the closed-loop system stability. Toward this end, it is essential to introduce the adaption or compensation mechanism for the sake of counteracting the uncertainty effect in the control developments. In particular, the immersion and invariance (I&I) technique has been an effective manner for the accurate estimation of uncertain parameters since it was proposed in [12]. The intuition behind such a methodology is to explore an adaptive law such that a prespecified estimation error manifold is attractive, in turn, guaranteeing the parameter estimation to its actual value. So far, various I&I adaption schemes have been developed for the accurate parameter estimation while completing the tracking objective of VTOL UAVs [13]–[16].

When it comes to the coordinated formation of multiple VTOL UAVs, it is intricate to extend the aforementioned control approaches for an individual directly due to the existence of information exchange. The conventional solutions to the coordinated formation issue, including the leader–follower-based approach [17], [18] and the virtual structure-based approach [19], [20], are in a centralized fashion. However, these approaches heavily depend on a central unit, leading to weak reliability arising from the potential central failure [21]. To overcome the dilemma caused by overcentralization, the distributed methodology, borrowing the idea from the consensus of multiagent systems [22]–[26], is available. In particular, a variety of distributed control algorithms has been proposed for the sake of the coordinated formation of multiple VTOL

Manuscript received July 14, 2019; revised April 24, 2020; accepted July 2, 2020. Date of publication August 10, 2020; date of current version May 19, 2022. This work was supported in part by the National Natural Science Foundation of China under Grant 61933001, Grant 61703229, and Grant 61806183; in part by the Fundamental Research Funds for the China Central Universities of USTB under Grant FRF-TP-19-018A3; in part by the Scientific and Technological Innovation Foundation of Shunde Graduate School under Grant BK19AE014; and in part by the Beijing Top Discipline for Artificial Intelligent Science and Engineering, University of Science and Technology Beijing. This article was recommended by Associate Editor Y. Shi. *(Corresponding author: Yao Zou.)*

The authors were with the School of Automation and Electrical Engineering, University of Science and Technology Beijing, Beijing 100083, China, and also with the Institute of Artificial Intelligence, University of Science and Technology Beijing, Beijing 100083, China (e-mail: zouyao@ustb.edu.cn; hjzhang@ustb.edu.cn; weihe@ieee.org).

Color versions of one or more figures in this article are available at https://doi.org/10.1109/TCYB.2020.3009404.

Digital Object Identifier 10.1109/TCYB.2020.3009404

UAVs. For example, a distributed controller was developed in [27] for the purpose of the concerned formation; and subsequently, two improved versions were proposed in [28] and [29] by considering additional linear velocity unavailability effect and intermittent as well as delayed communication effect. A nonsmooth consensus algorithm was proposed in [30] for the coordinated formation tracking. In [21], a distributed control algorithm was designed such that the intercollision was avoided during the reconfiguration progress. By introducing a connectivity maintenance mechanism, a distributed hierarchical control algorithm was put forward in [31] over a distance-based network topology. Moreover, by introducing a distributed observer to estimate the reference information, a distributed control algorithm was developed in [32] such that coordinated formation tracking was achieved. In addition, the coordinated formation issue of multiple VTOL UAVs was also studied in [33]–[35] over a switching topology. Nonetheless, the distributed schemes proposed in [21] and [27]–[35] are applicable under an indispensable hypothesis that no parametric uncertainties exist in the VTOL UAV system. This is unlikely to be guaranteed, in practice, suffering from measurement inaccuracy. On the other hand, although there have been various adaptive distributed protocols for multiagent systems subject to parametric uncertainties [36]–[39], they cannot be straightforwardly transferred to the underactuated VTOL UAVs.

This article investigates the coordinated formation control issue of heterogeneous VTOL UAVs with unavailable inertial parameters. In particular, an adaptive distributed control algorithm is developed under the cascaded structure. In the first place, an adaptive distributed command force introducing a saturation control strategy is synthesized in the position loop for the position formation, where an I&I adaption scheme is designed such that the exponential mass estimation is guaranteed. Such an I&I adaption scheme decouples the effect of the closed-loop position dynamics to the parameter estimation dynamics such that their stability is analyzed separately. Moreover, with an explicit bound of the mass estimation, a choice criterion of the control parameters is formulated such that a command attitude, together with an applied thrust, is extracted from the synthesized command force without singularity. Next, an adaptive applied torque is synthesized in the attitude loop for the attitude tracking to the command attitude. In terms of the Lyapunov theory, it is demonstrated that the proposed distributed control algorithm enables the VTOL UAVs to accomplish the concerned coordinated formation objective asymptotically. Compared with the previous works, the main contributions of this article are three-fold. To begin with, in contrast to the centralized control schemes in [17]–[20], a distributed control algorithm implementing local information exchange is developed herein for the coordinated formation control of multiple VTOL UAVs. However, unlike the distributed control algorithms in [21] and [27]–[35] for the coordinated formation of multiple VTOL UAVs with no uncertainty, the inertial parameters are unavailable and heterogeneous in this article. To preserve the desired accurate tracking in the case of parametric uncertainties, a feasible adaption scheme is introduced into the distributed control algorithm. On the other hand, rather than the conventional adaptive distributed control algorithms for the multiagent systems in [36]–[39], the proposed one introduces a saturation control strategy accompanied by an I&I adaptive scheme such that the nonsingular command attitude extraction is guaranteed according to an explicit choice criterion of the control parameters. Last but not least, compared with the I&I scheme presented in [13]–[16], the I&I adaption designed in this article guarantees the accurate mass estimation exponentially. This can determine a definite bound of the mass estimation for the sake of formulating the explicit choice criterion of the control parameters.

The remainder of this article is arranged as follows. Some preliminaries are provided in Section II. The problem to be solved is stated in Section III. The main results, including the control algorithm development and the stability analysis, are elaborated in Section IV. An illustrative example is simulated in Section V for the verification of the proposed control algorithm. A final conclusion is drawn in Section VI.

II. Preliminaries

In this section, some mathematical preliminaries are introduced for the convenience of the subsequent analysis.

A. Notations

Throughout this article, $\mathbb{R}$ denotes the real number set, $\mathbb{R}^n$ denotes the real vector set of dimension n, $\mathbb{R}^{m\times n}$ denotes the real matrix set of dimension $m \times n$; $|x|$ denotes the absolute value of $x \in \mathbb{R}$; $\|x\|$ denotes the Euclidean norm of $x \in \mathbb{R}^n$; $\|X\|$ denotes the Frobenius norm of $X \in \mathbb{R}^{m\times n}$; $\mathrm{tr}(Y)$, $\lambda_{\max}(Y)$, and $\lambda_{\min}(Y)$ denote the trace, maximum, and minimum eigenvalues of $Y \in \mathbb{R}^{n\times n}$; I_n is an identity matrix of $n \times n$; and $\mathrm{diag}\{x_1, x_2, \ldots, x_n\}$ denotes a diagonal matrix with its diagonal entries being x_1 to x_n. In addition, superscript $\times$ defines a transformation from $\mathbb{R}^3$ to $\mathbf{so} = \{C \in \mathbb{R}^{3\times 3} \mid C + C^T = 0\}$ and superscript $\vee$ defines its inverse operation.

B. Useful Results

Definition 1 [40]: A saturation function $\mathrm{sat}(x) : \mathbb{R} \to \mathbb{R}$ is an odd function with the following properties: 1) $x\mathrm{sat}(x) \geq 0$ and $\mathrm{sat}(x) = 0 \Leftrightarrow x = 0$; 2) $|\mathrm{sat}(x)| < \eta_a \; \forall x \in \mathbb{R}$; and 3) $\mathrm{dsat}(x) = \partial \mathrm{sat}(x)/\partial x \in (0, \eta_b]$, where η_a and η_b are positive bound constants.

Lemma 1 [35]: For $x \in \mathbb{R}^3$ and $M \in \mathbb{R}^{3\times 3}$, the following equalities hold:

$$\mathrm{tr}\left(x^\times M\right) = -x^T\left(M - M^T\right)^\vee \tag{1}$$

$$\left(x^\times M + M^T x^\times\right)^\vee = (\mathrm{tr}(M)I_3 - M)x. \tag{2}$$

C. Graph Theory

The network topology among VTOL UAVs is established by graph theory. In particular, a graph $\mathcal{G} \triangleq \{\mathcal{V}, \mathcal{E}\}$ consists of a node set $\mathcal{V} \triangleq \{1, 2, \ldots, n\}$ and an edge set $\mathcal{E} \subseteq \mathcal{V} \times \mathcal{V}$. For an undirected graph, $(i, j) \in \mathcal{E}$ indicates that node j and node i can exchange information with each other; and accordingly, node i (or j) is called a neighbor of node j (or i). All neighbors of node i are included in a set $\mathcal{N}_i = \{j \in \mathcal{V} \mid (j, i) \in \mathcal{E}\}$. A path from node i to node j is a sequence of edges. Moreover, an undirected graph is said to be connected if each node has a path to every other node.

For graph $\mathcal{G}$, its adjacency matrix $A = [a_{ij}] \in \mathbb{R}^{n\times n}$ is defined such that $a_{ij} > 0$ if $(j, i) \in \mathcal{E}$ and otherwise, $a_{ij} = 0$, and its Laplacian matrix $L = [l_{ij}] \in \mathbb{R}^{n\times n}$ is defined such that $l_{ii} = \sum_{j=1,j\neq i}^{n} a_{ij}$ and $l_{ij} = -a_{ij}$ for $j \neq i$. It is trivial that matrices A and L are symmetric for an undirected graph.

III. Problem Statement

A. System Model

Suppose that there is a VTOL UAV team of n members, labeled by $\mathcal{V} = \{1, 2, \dots, n\}$. Each of them is treated as a six-dof (i.e., degree of freedom) rigid body and operates in two reference frames: 1) a global inertia frame $\mathcal{I} \triangleq \{O_I x_I y_I z_I\}$ whose origin O_I is situated at the Earth center and 2) a local body frame $\mathcal{B} \triangleq \{O_B x_B y_B z_B\}$ whose origin O_B is in accordance with the UAV c.g. (i.e., center of gravity). In the context of modeling, a rotation matrix $R \in \mathrm{SO}(3) = \{R \in \mathbb{R}^{3\times 3} \mid R^T R = RR^T = I_3, \det R = 1\}$ is used to parameterize the rotation relation between two frames, that is, the UAV attitude. In particular, it characterizes a rotation of frame $\mathcal{I}$ by an Euler angle $\xi \in (-\pi, \pi]$ around an Euler axis $\hat{k} \in \mathbb{S}_2 = \{x \in \mathbb{R}^3 \mid \|x\| = 1\}$ to frame $\mathcal{B}$. Such a rotation relation can be explicitly determined by the Euler formula [41], that is

$$R = \cos\xi I_3 + (1 - \cos\xi)\hat{k}\hat{k}^T - \sin\xi \hat{k}^{\times}. \tag{3}$$

In addition, two useful equalities with regards to the rotation matrix are presented in the following lemmas.

Lemma 2 [35]: Given a rotation matrix $R \in \mathrm{SO}(3)$ with ξ being its Euler angle, the following equalities hold:

$$\left\| \frac{\left(R - R^T\right)^{\vee}}{2} \right\| = \cos\frac{\xi}{2}\sqrt{\mathrm{tr}(I_3 - R)} \tag{4}$$

$$\mathrm{tr}(I_3 - R) = 2(1 - \cos\xi). \tag{5}$$

Next, in terms of the Euler–Newton formula, the equation of motion of each VTOL UAV is formulated by

$$\dot{p}_i = v_i \tag{6}$$

$$\dot{v}_i = -g\hat{e}_3 + \frac{T_i}{m_i} R_i \hat{e}_3 \tag{7}$$

$$\dot{R}_i = R_i \omega_i^{\times} \tag{8}$$

$$J_i \dot{\omega}_i = -\omega_i^{\times} J_i \omega_i + \tau_i \tag{9}$$

where $p_i = [p_{i,x}, p_{i,y}, p_{i,z}]^T$ and $v_i = [v_{i,x}, v_{i,y}, v_{i,z}]^T$ denote the position and velocity of the UAV c.g. in frame $\mathcal{I}$, respectively, m_i is the total mass, g is the local gravitational acceleration, $\hat{e}_3 \triangleq [0, 0, 1]^T$, T_i denotes the applied thrust along $\hat{e}_3$, $\omega_i = [\omega_{i,x}, \omega_{i,y}, \omega_{i,z}]^T$ denotes the UAV angular velocity in frame $\mathcal{B}_i$, $J_i = \mathrm{diag}\{J_{i,x}, J_{i,y}, J_{i,z}\}$ denotes the inertia matrix with respect to frame $\mathcal{B}_i$, and τ_i denotes the applied torque in frame $\mathcal{B}_i$. Herein, $\mathcal{B}_i$ represents the body frame with respect to each VTOL UAV.

Remark 1: Typical VTOL UAVs incorporate quadrotor, helicopter, and ducted-fan aircraft in practice. Equations (6)–(9) can characterize their kinematics and dynamics except the mechanisms generating the applied thrust and torque. In the meantime, they are subject to distinct forms of aerodynamic disturbances in real flight scenarios [42], [43]. Actually, regardless of the aerodynamic and external disturbances, (6)–(9) can be treated as a nominal model for this class of VTOL UAVs. We focus on this nominal model in this article, while the proposed distributed control algorithm can be extended to the actual objects by using proper compensation schemes to address uncertainties.

B. Control Objective

Given a global reference velocity $v_r = [v_{r,x}, v_{r,y}, v_{r,z}]^T$, the concerned control objective in this article is to develop control thrust T_i and torque τ_i for each VTOL UAV such that they are capable of tracking the reference velocity while maintaining a prescribed formation pattern in a collaborative manner. Specifically, for $i, j \in \mathcal{V}$

$$\lim_{t\to\infty}\big(p_i(t) - p_j(t)\big) = \theta_{ij}, \quad \lim_{t\to\infty}(v_i(t) - v_r(t)) = 0 \tag{10}$$

where θ_{ij} is a desired position offset. It is essential to choose proper θ_{ij} so that a well-defined and unique formation pattern is available. However, the information interaction between different VTOL UAVs is a local subject to some ambient constraints in practice. Under such a circumstance, each individual has access to the interactive information just from its neighbors (including the desired position offset θ_{ij}). Besides, the concerned VTOL UAVs are heterogeneous with parametric uncertainties in the sense that their inertial parameters (i.e., masses and inertia matrices) are diverse and unavailable. To overcome the above dilemmas resulting from the local interaction constraint as well as the parametric heterogeneity and unavailability, an adaptive distributed control algorithm is to be developed. In what follows, we use an undirected graph $\mathcal{G} = \{\mathcal{V}, \mathcal{E}\}$ to characterize the network topology among the VTOL UAVs. In addition, to make the proposed control algorithm applicable, two fundamental assumptions are made as follows.

Assumption 1: The derivative of the reference velocity v_r satisfies $\sup_{t\geq 0} |\dot{v}_{r,z}| \leq \varrho < g$.

Assumption 2: The undirected graph $\mathcal{G}$ is connected.

IV. Main Results

The proposed adaptive distributed control algorithm for the coordinated formation control of a VTOL UAV team is based on a cascaded structure. Specifically, we first synthesize a command force for each UAV in the position loop for the sake of the position formation. Then, we evaluate a rotation matrix characterizing the orientation of each command force with respect to its corresponding body frame as a command attitude. Next, we synthesize an applied torque for each UAV in the attitude loop for the purpose of the attitude alignment with the command one. As a result of such an attitude alignment, the magnitude of the command force is exactly the applied thrust of interest. In terms of such a cascaded structure, the control algorithm is exploited according to the following procedure.

To begin with, the solution to the original coordinated formation problem of multiple VTOL UAVs is converted into solving a consensus problem of evolved error systems. Next, command forces are synthesized for the consensus of position error systems, and then applied torques are synthesized for the asymptotic stability of attitude error systems, where adaptive schemes are introduced to deal with the issue caused by the inertial parameter unavailability. Eventually, the stability analysis of the overall closed-loop error systems is elaborated according to the cascaded system stability theory.

A. Problem Conversion

First, define the position error $p_i^e = p_i - \int_0^t v_r(\sigma)\mathrm{d}\sigma - \theta_i$ and the velocity error $v_i^e = v_i - v_r$ for each UAV, where θ_i is a desired position offset with respect to the formation center. Note that $\theta_{ij} = \theta_i - \theta_j$ and further that $p_i^e - p_j^e = 0 \Leftrightarrow p_i - p_j = \theta_{ij}$, $i, j \in \mathcal{V}$. By virtue of (6) and (7), the ith position error system is derived as

$$\dot{p}_i^e = v_i^e \tag{11a}$$

$$\dot{v}_i^e = -g\hat{e}_3 - \dot{v}_r + \frac{u_i}{m_i} + \frac{T_i}{m_i}\left(R_i - R_i^c\right)\hat{e}_3 \tag{11b}$$

where $u_i = T_i R_i^c \hat{e}_3$ is a command force and $R_i^c \in \mathrm{SO}(3)$ is a command rotation matrix. Due to the fact that $\|R_i^c\hat{e}_3\| = 1$, once a command force u_i is determined, the applied thrust T_i is immediately derived as

$$T_i = \|u_i\|. \tag{12}$$

In order to make the applied thrust T_i along axis $\hat{e}_3$, it is necessary to adjust each attitude in alignment with the command rotation matrix R_i^c. Accordingly, we should first extract R_i^c from the command force u_i. For this purpose, in terms of the minimal rotation principle, the following lemma introduces a feasible extraction strategy.

Lemma 3 [44]: If the command force $u_i = [u_{i,x}, u_{i,y}, u_{i,z}]^T$, $i \in \mathcal{V}$ satisfies the nonsingular condition

$$u_i \notin \mathbb{U} = \left\{u \in \mathbb{R}^3 \mid u = \left[0, 0, u_z\right]^T, u_z \le 0\right\} \tag{13}$$

the command rotation matrix R_i^c can be extracted as

$$R_i^c = \frac{1}{\|u_i\|}\begin{bmatrix} u_{i,z} + \frac{u_{i,y}^2}{\|u_i\|+u_{i,z}} & -\frac{u_{i,x}u_{i,y}}{\|u_i\|+u_{i,z}} & u_{i,x} \\ -\frac{u_i^x u_i^y}{\|u_i\|+u_i^z} & u_{i,z} + \frac{u_{i,y}^2}{\|u_i\|+u_{i,z}} & u_{i,y} \\ -u_{i,x} & -u_{i,y} & u_{i,z} \end{bmatrix}. \tag{14}$$

Suppose that the command rotation matrix R_i^c has been evaluated. We next define the attitude error $R_i^e = (R_i^c)^T R_i$ for $i \in \mathcal{V}$. Note that $R_i^e = I_3$ implies that $R_i = R_i^c$, that is, the exact attitude tracking [41]. By virtue of (8), it can be derived that R_i^e satisfies the following dynamics:

$$\dot{R}_i^e = R_i^e\left(\omega_i^e\right)^\times \tag{15}$$

where $\omega_i^e = \omega_i - (R_i^e)^T\omega_i^c$ is the angular velocity error with ω_i^c being the command angular velocity. The explicit expressions of the command angular velocity ω_i^c and its derivative $\dot{\omega}_i^c$ are given in the Appendix. Refer to [44] for their detailed derivations. Similarly, R_i^e complies with the Euler formula (3) with Euler angle $\xi_i^e \in (-\pi, \pi]$ and axis $\hat{k}_i^e \in \mathbb{S}_2$. Moreover, in terms of Lemma 1, it follows that:

$$\mathrm{tr}\left(\dot{R}_i^e\right) = -\mathrm{tr}\left(\left(\omega_i^e\right)^\times\left(R_i^e\right)^T\right) = -\varepsilon_i^T\omega_i^e \tag{16}$$

where $\varepsilon_i = (R_i^e - (R_i^e)^T)^\vee$. According to Lemma 2, $\varepsilon_i = 0$ indicates that $R_i^e = I_3$ or $\xi_i^e = \pi$, but $\xi_i^e = \pi$ is undesired. In addition, in terms of (15) and Lemma 1, the derivative of ε_i satisfies

$$\dot{\varepsilon}_i = \left(R_i^e\left(\omega_i^e\right)^\times + \left(\omega_i^e\right)^\times R_i^e\right)^\vee = \Omega_i\omega_i^e \tag{17}$$

where $\Omega_i = \mathrm{tr}(R_i^e)I_3 - R_i^e$ satisfies

$$\|\Omega_i\| = \sqrt{\mathrm{tr}\left(\Omega_i^T\Omega_i\right)} = \sqrt{3 + \mathrm{tr}\left(R_i^e\right)^2} \le 2\sqrt{3}. \tag{18}$$

Next, it follows from (9) and (15) that ω_i^e satisfies the following dynamics:

$$\begin{aligned} J_i\dot{\omega}_i^e &= -\omega_i^\times J_i\omega_i + \tau_i + J_i\left[\left(\omega_i^e\right)^\times\left(R_i^e\right)^T\omega_i^c - \left(R_i^e\right)^T\dot{\omega}_i^c\right] \\ &= \tau_i + \Gamma_i\rho_i \end{aligned} \tag{19}$$

where $\rho_i = [J_{i,x}, J_{i,y}, J_{i,z}]^T$ and

$$\Gamma_i = \begin{bmatrix} \varpi_{i,x} & \omega_{i,y}\omega_{i,z} & -\omega_{i,y}\omega_{i,z} \\ -\omega_{i,x}\omega_{i,z} & \varpi_{i,y} & \omega_{i,x}\omega_{i,z} \\ \omega_{i,x}\omega_{i,y} & -\omega_{i,x}\omega_{i,y} & \varpi_{i,z} \end{bmatrix}$$

with $\varpi_i = [\varpi_{i,x}, \varpi_{i,y}, \varpi_{i,z}]^T = (\omega_i^e)^\times(R_i^e)^T\omega_i^c - (R_i^e)^T\dot{\omega}_i^c$.

Note that from the above analysis, the coordinated formation problem for a team of VTOL UAVs (6)–(8) can be converted into the consensus problem of evolved error systems (11), (15), and (19). The following lemma indicates this point.

Lemma 4: For the ith error system (11), (15), and (19), if a command force u_i and an applied torque τ_i can be synthesized such that

$$\begin{aligned} \lim_{t\to\infty}\left(p_i^e(t) - p_j^e(t)\right) = 0, \quad \lim_{t\to\infty} v_i^e(t) = 0 \\ \lim_{t\to\infty} R_i^e(t) = I_3, \quad \lim_{t\to\infty}\omega_i^e(t) = 0 \end{aligned} \tag{20}$$

$\forall i, j \in \mathcal{V}$, the coordinated formation control of a team of VTOL UAVs (6)–(9) is achieved in the sense of (10).

Remark 2: As will be shown subsequently, the proposed distributed control algorithm is in fact dependent on the relative position offset θ_{ij} rather than the absolute one δ_i. The introduction of δ_i just plays a role in facilitating the analysis. Toward this end, the formation center is unnecessarily available to each VTOL UAV in practice.

B. Command Force Development

For the sake of the nonsingular condition (13), we consider implementing a saturation control strategy for the command force development. Moreover, an I&I adaptive algorithm is designed to address the problem caused by mass unavailability.

First, for each VTOL UAV, define a filtered error as follows:

$$s_i = c_p\sum_{j\in\mathcal{N}_i} a_{ij}\left(p_i - p_j - \theta_{ij}\right) + v_i^e \tag{21}$$

where c_p is a positive parameter and a_{ij} is the (i,j)th entry of the adjacency matrix A associated with graph $\mathcal{G}$. The derivative of s_i along (11) satisfies

$$\begin{aligned}\dot{s}_i &= c_p \sum_{j\in\mathcal{N}_i} a_{ij}\big(v_i - v_j\big) - g\hat{e}_3 - \dot{v}_r + \frac{u_i}{m_i} + \frac{T_i}{m_i}\big(R_i - R_i^c\big)\hat{e}_3 \\ &= c_p \sum_{j=1}^{n} a_{ij}\Big(v_i^e - v_j^e\Big) - \big(g\hat{e}_3 + \dot{v}_r\big) + \frac{u_i}{m_i} + \frac{T_i}{m_i}\big(R_i - R_i^c\big)\hat{e}_3.\end{aligned} \tag{22}$$

By using a saturation control strategy, the proposed command force for each VTOL UAV is in the following form:

$$u_i = \frac{\alpha_m \hat{m}_i}{\phi_i}\Big[-\alpha_p\big(\mathrm{sat}(s_i) + \mathrm{sat}\big(v_i^e\big)\big) + g\hat{e}_3 + \dot{v}_r\Big] \tag{23}$$

where α_m and α_p are positive control parameters, $\hat{m}_i$ is an estimation of m_i, $\mathrm{sat}(\cdot)$ is some saturation function given in Definition 1 with a bound constant σ_a, and $\phi_i = 2 + \sum_{k=x,y,z} \mathrm{sat}(v_{i,k})/(3\sigma_a) > 1$. In addition, $\hat{m}_i$ is updated by the I&I adaptive algorithm in the following form:

$$\dot{\hat{m}}_i = -\frac{-g\mathrm{dsat}\big(v_{i,z}\big)}{3\sigma_a\phi_i}\hat{m}_i + \frac{T_i}{3\sigma_a\alpha_m}\zeta_i^T R_i\hat{e}_3 \tag{24}$$

where $\zeta_i = [\mathrm{dsat}(v_{i,x}), \mathrm{dsat}(v_{i,y}), \mathrm{dsat}(v_{i,z})]^T$. Note that from (23) and (24), in order for the implementation of the proposed command force, each UAV needs to have access to its neighboring position information.

Next, recall the nonsingular condition (13). It is trivial that $u_{i,z} > 0$ is sufficient for $u_i \notin \mathbb{U}$. For this purpose, we choose the control parameter $\alpha_p < (g - \varrho)/(2\sigma_a)$ given in Assumption 1. In such a case, if $\hat{m}_i > 0$ is guaranteed, the third row of (23) satisfies

$$u_{i,z} > \alpha_m \inf_{t\geq 0}\left\{\frac{\hat{m}_i(t)}{\phi_i(t)}\right\}\big(g - \varrho - 2\alpha_p\sigma_a\big) > 0. \tag{25}$$

Hence, $u_i \notin \mathbb{U}$, $i \in \mathcal{V}$, that is, no singularity occurs. In the subsequent stability analysis part, we will show that the adaptive law (24) ensures each $\hat{m}_i(t) > 0$, $\forall t \geq 0$. Accordingly, such a parameter criterion is sufficient for singularity avoidance.

Remark 3: Note from (23) that the developed command force in terms of a saturated control strategy is in a node-based distributed manner [45]. In contrast to the edge-based manner [22], the interaction component as a whole can be the argument of the saturation function herein so that the choice of the control parameter α_p is irrelative to the graph weight a_{ij} any more.

C. Applied Torque Development

As described earlier, $\varepsilon_i = 0$ implies that $R_i^e = I_3$ or $\xi_i^e = \pi$, whereas only $R_i^e = I_3$ is desired. Based on Lemma 2, it follows that $\mathrm{tr}(I_3 - R_i^e) \in [0,4]$ and that $\xi_i^e = \pi$ is equivalent to $\mathrm{tr}(I_3 - R_i^e) = 4$. Hence, if an applied torque τ_i can be developed such that $\lim_{t\to\infty}\varepsilon(t) = 0$ and $\lim_{t\to\infty}\omega_i^e(t) = 0$ with $\mathrm{tr}(I_3 - R_i^e) \in [0,4)$, the concerned attitude tracking objective is achieved.

In particular, the proposed applied torque for each VTOL UAV is in the following form:

$$\tau_i = -\frac{\varepsilon_i}{4 - \mathrm{tr}\big(I_3 - R_i^e\big)} - \alpha_\varepsilon\varepsilon_i - \alpha_\omega\omega_i^e - \Gamma_i\hat{\rho}_i \tag{26}$$

where α_ε and α_ω are positive control parameters and $\hat{\rho}_i = [\hat{J}_{i,x}, \hat{J}_{i,y}, \hat{J}_{i,z}]^T$ is an estimation of ρ_i. The adaptive law for each $\hat{\rho}_i$ is designed as

$$\dot{\hat{\rho}}_i = \alpha_\rho\Gamma_i^T\big(c_\varepsilon\varepsilon_i + \omega_i^e\big) \tag{27}$$

where α_ρ and c_ε are positive adaptive parameters.

Remark 4: Note that from (26) and (27), to implement the proposed applied torque τ_i, the command angular velocity ω_i^c and its derivative $\dot{\omega}_i^c$ should be available. According to the Appendix, they are determined by the derivatives of the command force u_i. However, it is intricate to formulate explicit expressions of $\dot{u}_i$ and $\ddot{u}_i$. Alternatively, inspired by [46], a high-order Levant differentiator is introduced to estimate them. In particular

$$\begin{aligned}&\dot{\kappa}_{i,k} = \delta_{i,k}, \quad \delta_{i,k} = -\lambda_0\big|\kappa_{i,k} - u_{i,k}\big|^{\frac{2}{3}}\mathrm{sign}\big(\kappa_{i,k} - u_{i,k}\big) + \delta'_{i,k} \\ &\dot{\kappa}'_{i,k} = \delta'_{i,k}, \quad \delta'_{i,k} = -\lambda_1\big|\kappa'_{i,k} - \delta_{i,k}\big|^{\frac{1}{2}}\mathrm{sign}\big(\kappa'_{i,k} - \delta_{i,k}\big) + \kappa''_{i,k} \\ &\dot{\kappa}''_{i,k} = -\lambda_2\mathrm{sign}\big(\kappa''_{i,k} - \delta'_{i,k}\big), \quad k = x, y, z\end{aligned} \tag{28}$$

where $\kappa_i = [\kappa_{i,x}, \kappa_{i,y}, \kappa_{i,z}]^T$, $\kappa'_i = [\kappa'_{i,x}, \kappa'_{i,y}, \kappa'_{i,z}]^T$, and $\kappa''_i = [\kappa''_{i,x}, \kappa''_{i,y}, \kappa''_{i,z}]^T$ are the estimations of u_i, $\dot{u}_i$, and $\ddot{u}_i$, respectively, and λ_0, λ_1, and λ_2 are positive constants. According to [46], by properly specifying λ_0, λ_1, and λ_2, κ_i, κ'_i, and κ''_i are capable of accurately estimating u_i, $\dot{u}_i$, and $\ddot{u}_i$ in finite time. Moreover, provided that the estimation dynamics (28) is of a faster convergence rate than that of the closed-loop attitude system, such estimations make no difference to the stable performance of the overall closed-loop system.

D. Stability Analysis

In this section, we intend to show the achievement of the coordinated formation control of a team of heterogeneous VTOL UAVs in the presence of parametric uncertainties by using the proposed adaptive distributed control algorithm. The underlying analysis is carried out under the cascaded structure. In particular, we first show the asymptotic stability of the attitude error system driven by the proposed applied torque (26). Then, we show the exponential estimation of the mass updated by the I&I adaptive algorithm (24). With these two results, we next show the asymptotic consensus of the position error system driven by the proposed command force (23). Finally, a theorem is provided to summarize the overall stability result.

In the first place, Proposition 1 shows that the proposed applied torque (26) guarantees the asymptotic stability of the attitude error system (15) and (19).

Proposition 1: Consider the ith attitude error system (15) and (19). Given $\mathrm{tr}(I_3 - R_i^e(0)) \neq 4$ and

$$c_\varepsilon < \min\left\{\sqrt{\frac{\alpha_\varepsilon}{2\bar{J}}}, \frac{2\sqrt{3}\bar{J}}{\alpha_\omega}, \frac{4\alpha_\varepsilon\alpha_\omega}{\alpha_\omega^2 + 8\sqrt{3}\alpha_\varepsilon c_\varepsilon\bar{J}}\right\}$$

with $\bar{J} = \max_{i\in\mathcal{V}}\{\lambda_{\max}(J_i)\}$, the developed applied torque (26) with adaptive law (27) guarantees that $\lim_{t\to\infty} R_i^e(t) = I_3$ and $\lim_{t\to\infty}\omega_i^e(t) = 0$, $i \in \mathcal{V}$.

Proof: For each $i \in \mathcal{V}$, assign a Lyapunov function as follows:

$$L_i^a = \ln\frac{4}{4-\mathrm{tr}\left(I_3 - R_i^e\right)} + \alpha_\varepsilon\left(4 - \mathrm{tr}\left(I_3 - R_i^e\right)\right) + c_\varepsilon\varepsilon_i^T J_i\omega_i^e + \frac{1}{2}\left(\omega_i^e\right)^T J_i\omega_i^e + \frac{1}{2\alpha_\rho}\tilde{\rho}_i^T\tilde{\rho}_i \tag{29}$$

where $\tilde{\rho}_i = \hat{\rho}_i - \rho_i$ is the estimation error. It follows from Lemma 2 that $4 - \mathrm{tr}(I_3 - R_i^e) \geq \|\varepsilon_i\|^2/4$. Thus, L_i^a satisfies $L_i^a \geq \gamma_i^T W_i\gamma_i$, where $\gamma_i = [\varepsilon_i^T, (\omega_i^e)^T, \tilde{\rho}_i^T]^T$ and matrix

$$W_i = \begin{bmatrix} \frac{\alpha_\varepsilon}{4}I_3 & \frac{c_\varepsilon}{2}J_i & 0 \\ \frac{c_\varepsilon}{2}J_i & \frac{1}{2}J_i & 0 \\ 0 & 0 & \frac{1}{2\alpha_\rho}I_3 \end{bmatrix}$$

is positive definite given that $c_\varepsilon < \sqrt{\alpha_\varepsilon/(2\bar{J})}$. Next, by considering (16)–(19), its derivative satisfies

$$\begin{aligned}\dot{L}_i^a &= \frac{\varepsilon_i^T\omega_i^e}{4-\mathrm{tr}\left(I_3 - R_i^e\right)} + \alpha_\varepsilon\varepsilon_i^T\omega_i^e + c_\varepsilon\left(\omega_i^e\right)^T\Omega_i^T J_i\omega_i^e \\ &\quad + \left(c_\varepsilon\varepsilon_i + \omega_i^e\right)^T(\tau_i + \Gamma_i\rho_i) + \frac{1}{\alpha_\rho}\tilde{\rho}_i^T\dot{\hat{\rho}}_i \\ &\leq \frac{\varepsilon_i^T\omega_i^e}{4-\mathrm{tr}\left(I_3 - R_i^e\right)} + \alpha_\varepsilon\varepsilon_i^T\omega_i^e + 2\sqrt{3}c_\varepsilon\bar{J}\left\|\omega_i^e\right\|^2 \\ &\quad + \left(c_\varepsilon\varepsilon_i + \omega_i^e\right)^T(\tau_i + \Gamma_i\rho_i) + \frac{1}{\alpha_\rho}\tilde{\rho}_i^T\dot{\hat{\rho}}_i.\end{aligned} \tag{30}$$

Substituting the proposed applied torque (26) into (30) yields

$$\begin{aligned}\dot{L}_i^a &\leq -\frac{c_\varepsilon\|\varepsilon_i\|^2}{4-\mathrm{tr}\left(I_3 - R_i^e\right)} - c_\varepsilon\alpha_\varepsilon\|\varepsilon_i\|^2 - \left(\alpha_\omega - 2\sqrt{3}c_\varepsilon\bar{J}\right)\left\|\omega_i^e\right\|^2 \\ &\quad - c_\varepsilon\alpha_\omega\varepsilon_i^T\omega_i^e + \frac{1}{\alpha_\rho}\tilde{\rho}_i^T\left(\dot{\hat{\rho}}_i - \alpha_\rho\Gamma_i^T\left(c_\varepsilon\varepsilon_i + \omega_i^e\right)\right).\end{aligned} \tag{31}$$

By further substituting the adaptive law (27) into (31), it follows that:

$$\begin{aligned}\dot{L}_i^a &\leq -c_\varepsilon\alpha_\varepsilon\|\varepsilon_i\|^2 - \left(\alpha_\omega - 2\sqrt{3}c_\varepsilon\bar{J}\right)\left\|\omega_i^e\right\|^2 - c_\varepsilon\alpha_\omega\varepsilon_i^T\omega_i^e \\ &= -\bar{z}_i^T\bar{W}_i\bar{z}_i\end{aligned} \tag{32}$$

where $\bar{z}_i = [\varepsilon_i^T, (\omega_i^e)^T]^T$ and matrix

$$\bar{W}_i = \begin{bmatrix} c_\varepsilon\alpha_\varepsilon I_3 & \frac{c_\varepsilon\alpha_\omega}{2}I_3 \\ \frac{c_\varepsilon\alpha_\omega}{2}I_3 & \left(\alpha_\omega - 2\sqrt{3}c_\varepsilon\bar{J}\right)I_3 \end{bmatrix}$$

is positive definite if $c_\varepsilon < \min\{2\sqrt{3}\bar{J}/\alpha_\omega, 4\alpha_\varepsilon\alpha_\omega/(\alpha_\omega^2 + 8\sqrt{3}\alpha_\varepsilon c_\varepsilon\bar{J})\}$. It thus follows that:

$$\dot{L}_i^a \leq -\lambda_{\min}\left(\bar{W}_i\right)\|\bar{z}_i\|^2. \tag{33}$$

According to the comparison principal [47], it follows that:

$$L_i^a(t) + \lambda_{\min}\left(\bar{W}_i\right)\int_0^\infty\|\bar{z}_i(\sigma)\|^2\mathrm{d}\sigma \leq L_i^a(0) \quad \forall t \geq 0. \tag{34}$$

This implies that $L_i^a \in \mathbb{L}_\infty$[1] and $\bar{z}_i$ (or $\varepsilon_i, \omega_i^e$) $\in \mathbb{L}_2$.[2] It follows from (29) that $\ln(4/(4 - \mathrm{tr}(I_3 - R_i^e)))$, ω_i^e, $\tilde{\rho}_i$ (or $\hat{\rho}_i$) $\in \mathbb{L}_\infty$. Thus, as long as $R_i^e(0)$ satisfies $\mathrm{tr}(I_3 - R_i^e(0)) < 4$, then $\mathrm{tr}(I_3 - R_i^e(t)) < 4$ and further $\xi_i^e(t) \neq \pi$ $\forall t \geq 0$ can be guaranteed. In addition, it follows from (17) and (19) that $\dot{\varepsilon}_i, \dot{\omega}_i^e \in \mathbb{L}_\infty$. According to the Barbalat lemma [47], it follows that $\lim_{t\to\infty}\varepsilon_i(t) = 0$ and $\lim_{t\to\infty}\omega_i^e(t) = 0$, $i \in \mathcal{V}$. Since $\xi_i^e \neq \pi$ has been guaranteed, this finally implies that $\lim_{t\to\infty} R_i^e(t) = I_3$, $i \in \mathcal{V}$. ■

[1] $\mathbb{L}_\infty = \{f : \mathbb{R}^+ \to \mathbb{R}^n | f$ is locally integrable, $\mathrm{ess\,sup}_{t\in\mathbb{R}^+}\|f(t)\| < \infty\}$.

[2] $\mathbb{L}_2 = \{f : \mathbb{R}^+ \to \mathbb{R}^n | f$ is locally integrable, $\int_0^\infty\|f(t)\|^2\mathrm{d}t < \infty\}$.

In the second place, Proposition 2 shows that the proposed I&I adaptive algorithm (24) guarantees the accurate estimation of each mass with exponential convergence performance.

Proposition 2: If each initial mass estimation $\hat{m}_i(0) \geq (\phi_i(0) - 1)\bar{m}/\alpha_m$, where $\bar{m} \geq m_i$ is a bound constant, the developed adaptive algorithm (24) guarantees that: 1) $\lim_{t\to\infty}\alpha_m\hat{m}_i(t)/\phi_i(t) = m_i$, $i \in \mathcal{V}$ and 2) $0 < \alpha_m\hat{m}_i(t)/\phi_i(t) \leq \alpha_m\hat{m}_i(0) + \bar{m}$ $\forall t \geq 0$, $i \in \mathcal{V}$.

Proof:

1) For $i \in \mathcal{V}$, define the estimation error

$$\tilde{m}_i = \alpha_m\hat{m}_i - \phi_i m_i. \tag{35}$$

It follows from (7) that the derivative of each $\tilde{m}_i$ satisfies:

$$\begin{aligned}\dot{\tilde{m}}_i &= \alpha_m\dot{\hat{m}}_i - \frac{1}{3\sigma_a}\zeta_i^T\left(-m_i g\hat{e}_3 + T_i R_i\hat{e}_3\right) \\ &= \alpha_m\dot{\hat{m}}_i - \frac{1}{3\sigma_a}\zeta_i^T\left(\frac{\tilde{m}_i - \alpha_m\hat{m}_i}{\phi_i}g\hat{e}_3 + T_i R_i\hat{e}_3\right).\end{aligned} \tag{36}$$

Substituting the adaptive law (24) into (36), $\dot{\tilde{m}}_i$ further satisfies

$$\dot{\tilde{m}}_i = -\frac{g\mathrm{dsat}\left(v_{i,z}\right)}{3\sigma_a\phi_i}\tilde{m}_i. \tag{37}$$

For each $i \in \mathcal{V}$, assign a Lyapunov function $L_i^m = \tilde{m}_i^2/2$. Due to the facts that $\mathrm{dsat}(v_{i,z}) > 0$ and $\phi_i > 1$, its derivative along (37) satisfies $\dot{L}_i^m \leq -\inf\{2g\mathrm{dsat}(v_{i,z})/(3\sigma_a\phi_i)\}L_i^m$. This implies that each estimation error $\tilde{m}_i$ is exponentially stable, that is, $\lim_{t\to\infty}\tilde{m}_i(t) = 0$, $i \in \mathcal{V}$. By virtue of (35), it thus follows that $\lim_{t\to\infty}\alpha_m\hat{m}_i(t)/\phi_i(t) = m_i$, $i \in \mathcal{V}$.

2) The next analysis is divided into two cases depending on the sign of $\tilde{m}_i(0)$.

Case I [$\tilde{m}_i(0) \geq 0$]: In such a case, we have that $0 \leq \tilde{m}_i(t) \leq \tilde{m}_i(0)$ $\forall t \geq 0$ given the exponential stability of $\tilde{m}_i$. It then follows from (35) that $\alpha_m\hat{m}_i/\phi_i = m_i + \tilde{m}_i/\phi_i > 0$ and that:

$$\frac{\alpha_m\hat{m}_i}{\phi_i} \leq \frac{\tilde{m}_i(0)}{\phi_i} + m_i = \frac{\alpha_m\hat{m}_i(0)}{\phi_i} + \left(1 - \frac{\phi_i(0)}{\phi_i}\right)m_i. \tag{38}$$

Due to the fact that $\phi_i > 1$, it follows that $\alpha_m\hat{m}_i(t)/\phi_i(t) \leq \alpha_m\hat{m}_i(0) + \bar{m}$ $\forall t \geq 0$.

Case II [$\tilde{m}_i(0) < 0$]: In such a case, we have that $\tilde{m}_i(0) \leq \tilde{m}_i(t) \leq 0$ $\forall t \geq 0$ given the exponential stability of $\tilde{m}_i$. By considering (35), it follows that $\alpha_m\hat{m}_i/\phi_i = m_i + \tilde{m}_i/\phi_i < m_i \leq \alpha\hat{m}_i(0) + \bar{m}$. Next, due to the fact that $\phi_i > 1$, if $\hat{m}_i(0) \geq (\phi_i(0) - 1)\bar{m}/\alpha_m$, it follows from (35) that:

$$\begin{aligned}\frac{\alpha_m\hat{m}_i}{\phi_i} &\geq \frac{\tilde{m}_i(0)}{\phi_i} + m_i \geq \tilde{m}_i + m_i \\ &= \alpha_m\hat{m}_i(0) + (1-\phi_i(0))m_i \\ &> (\phi_i(0)-1)(\bar{m}-m_i) \geq 0. \end{aligned}\tag{39}$$

Therefore, it follows from the above argument that if $\hat{m}_i(0) \geq (\phi_i(0)-1)\bar{m}/\alpha_m$, then $0 < \alpha_m\hat{m}_i(t)/\phi_i(t) \leq \alpha_m\hat{m}_i(0) + \bar{m}\ \forall t \geq 0,\ i \in \mathcal{V}$. ■

Remark 5: It follows from Proposition 2, (12), and (23) that the resulting applied thrust T_i, $i \in \mathcal{V}$ is bounded by:

$$T_i \leq \left(\alpha_m\hat{m}_i(0) + \bar{m}\right)\left(2\sqrt{3}\alpha_p\sigma_1 + g + \sup_{t\geq 0}\|\dot{v}_r\|\right).\tag{40}$$

This inequality relation could be a criterion for selecting the control parameter α_p, the initial estimation $\hat{m}_i(0)$, and the reference velocity v_r such that the derived applied thrust is maintained without exceeding its maximum value. Moreover, the inequality (40) plays an important role in the stability analysis of the position error loop as shown in Proposition 3.

In the third place, in terms of Propositions 1 and 2, Proposition 3 shows that the proposed command force (23) guarantees the asymptotic consensus of the position error system (11).

Proposition 3: Consider the ith position error system (11). Suppose that Assumptions 1 and 2 hold. If $\lim_{t\to\infty} R_i^e(t) = I_3$ and $\lim_{t\to\infty}\tilde{m}_i(t) = 0$, $i \in \mathcal{V}$ are achieved, the proposed command force (23) guarantees that $\lim_{t\to\infty}(p_i^e(t) - p_j^e(t)) = 0$ and $\lim_{t\to\infty} v_i^e(t) = 0$, $i, j \in \mathcal{V}$.

Proof: First, by substituting the proposed command force (23) into (22) and (42), it follows that:

$$\dot{s}_i = c_p\sum_{j=1}^n a_{ij}\left(v_i^e - v_j^e\right) - \alpha_p\left(\mathrm{sat}(s_i) + \mathrm{sat}\left(v_i^e\right)\right) + \psi_i \tag{41a}$$

$$\dot{v}_i^e = -\alpha_p\left(\mathrm{sat}(s_i) + \mathrm{sat}\left(v_i^e\right)\right) + \psi_i \tag{41b}$$

where $\psi_i = \psi_{i,1} + \psi_{i,2}$ with $\psi_{i,1} = T_i(R_i - R_i^c)\hat{e}_3/m_i$ and $\psi_{i,2} = -\tilde{m}_i[-\alpha_p(\mathrm{sat}(s_i) + \mathrm{sat}(v_i^e)) + g\hat{e}_3 + \dot{v}_r]/(\phi_i m_i)$. Note that the closed-loop position error system (41) can be treated as a nominal system

$$\dot{s}_i = c_p\sum_{j=1}^n a_{ij}\left(v_i^e - v_j^e\right) - \alpha_p\left(\mathrm{sat}(s_i) + \mathrm{sat}\left(v_i^e\right)\right) \tag{42a}$$

$$\dot{v}_i^e = -\alpha_p\left(\mathrm{sat}(s_i) + \mathrm{sat}\left(v_i^e\right)\right) \tag{42b}$$

perturbed by ψ_i. According to the input-to-state theory [47], the asymptotic stability of the closed-loop position error system (41) can be guaranteed by: 1) $\lim_{t\to\infty}\psi_i(t) = 0$, $i \in \mathcal{V}$ and 2) the asymptotic stability of the nominal system (42). By following this idea, the subsequent proof is divided into two steps.

Step I: We first focus on the perturbation ψ_i, $i \in \mathcal{V}$. In terms of Proposition 2, (12), and the fact that $\|R_i^c\hat{e}_3\| = \|R_i\hat{e}_3\| = 1$, it follows that:

$$\|\psi_{i,1}\| \leq \frac{\sqrt{2}\left(\alpha_m\hat{m}_i(0) + \bar{m}\right)}{m_i}\left(2\sqrt{3}\alpha_p\sigma_1 + g + \sup_{t\geq 0}\|\dot{v}_r(t)\|\right)$$

$$\|\psi_{i,2}\| \leq \frac{\tilde{m}_i(0)}{m_i}\left(2\sqrt{3}\alpha_p\sigma_1 + g + \sup_{t\geq 0}\|\dot{v}_r(t)\|\right).$$

Therefore, $\psi_{i,1}$ and $\psi_{i,2}$, $i \in \mathcal{V}$ are bounded. Based on this result, the conditions that $\lim_{t\to\infty} R_i^e(t) = I_3$ and $\lim_{t\to\infty}\tilde{m}_i(t) = 0$ guarantee that $\lim_{t\to\infty}\psi_{i,1}(t) = 0$ and $\lim_{t\to\infty}\psi_{i,2}(t) = 0$, $i \in \mathcal{V}$. These indicate that $\lim_{t\to\infty}\psi_i(t) = 0$, $i \in \mathcal{V}$.

Step II: We next focus on the nominal system (42). Assign a Lyapunov function as follows:

$$L^p = \sum_{i=1}^n\left(\int_0^{s_i}\mathrm{sat}(\chi)^T\mathrm{d}\chi + \int_0^{v_i^e}\mathrm{sat}(\chi)^T\mathrm{d}\chi \times \frac{c_p}{4\alpha_p}\sum_{j=1}^n a_{ij}\left\|v_i^e - v_j^e\right\|^2\right).\tag{43}$$

Its derivative along (42) satisfies

$$\begin{aligned}\dot{L}^p &= \sum_{i=1}^n\left[c_p\mathrm{sat}(s_i)^T\sum_{j=1}^n a_{ij}\left(v_i^e - v_j^e\right)\right] \\ &\quad + \sum_{i=1}^n\left[\mathrm{sat}(s_i) + \mathrm{sat}\left(v_i^e\right)\right]^T\dot{v}_i^e \\ &\quad + \frac{c_p}{2\alpha_p}\sum_{i=1}^n\sum_{j=1}^n a_{ij}\left(v_i^e - v_j^e\right)^T\left(\dot{v}_i^e - \dot{v}_j^e\right).\end{aligned}\tag{44}$$

Given Assumption 2, it is trivial to show that

$$\sum_{i=1}^n\sum_{j=1}^n a_{ij}\left(v_i^e - v_j^e\right)^T\left(\dot{v}_i^e - \dot{v}_j^e\right) = 2\sum_{i=1}^n\sum_{j=1}^n a_{ij}\left(v_i^e - v_j^e\right)^T\dot{v}_i^e.\tag{45}$$

It thus follows that:

$$\begin{aligned}\dot{L}^p &= \sum_{i=1}^n\left[c_p\mathrm{sat}(s_i)^T\sum_{j=1}^n a_{ij}\left(v_i^e - v_j^e\right)\right] \\ &\quad + \sum_{i=1}^n\left[\mathrm{sat}(s_i) + \mathrm{sat}\left(v_i^e\right) + \frac{c_p}{\alpha_p}\sum_{i=1}^n\sum_{j=1}^n a_{ij}\left(v_i^e - v_j^e\right)\right]^T \\ &\quad \times\left[-\alpha_p\left(\mathrm{sat}(s_i) + \mathrm{sat}\left(v_i^e\right)\right)\right] \\ &= -\alpha_p\sum_{i=1}^n\left\|\mathrm{sat}(s_i) + \mathrm{sat}\left(v_i^e\right)\right\|^2 \\ &\quad - c_p\sum_{i=1}^n\sum_{j=1}^n a_{ij}\left(v_i^e - v_j^e\right)^T\mathrm{sat}\left(v_i^e\right).\end{aligned}\tag{46}$$

Next, by considering Assumption 2 and using the increasing property of the saturation function $\mathrm{sat}(\cdot)$, it is not hard to verify that

$$\begin{aligned}&\sum_{i=1}^n\sum_{j=1}^n a_{ij}\left(v_i^e - v_j^e\right)^T\mathrm{sat}\left(v_i^e\right) \\ &\quad = \frac{1}{2}\sum_{i=1}^n\sum_{j=1}^n a_{ij}\left(v_i^e - v_j^e\right)^T\left[\mathrm{sat}\left(v_i^e\right) - \mathrm{sat}\left(v_j^e\right)\right] \geq 0.\end{aligned}\tag{47}$$

Hence, $\dot{L}^p$ further satisfies

$$\dot{L}^p \leq -\alpha_p \sum_{i=1}^{n} \left\| \mathrm{sat}(s_i) + \mathrm{sat}\left(v_i^e\right) \right\|^2. \tag{48}$$

According to the comparison principal [47], it follows that:

$$\begin{aligned} &L^p(t) + \alpha_p \sum_{i=1}^{n} \int_0^{\infty} \left\| \mathrm{sat}(s_i(\sigma)) + \mathrm{sat}\left(v_i^e(\sigma)\right) \right\|^2 \mathrm{d}\sigma \\ &\leq L^p(0) \quad \forall t \geq 0. \end{aligned} \tag{49}$$

This implies that $(\mathrm{sat}(s_i) + \mathrm{sat}(v_i^e)) \in \mathbb{L}_2$, $i \in \mathcal{V}$. Moreover, it is obvious that $(\mathrm{sat}(s_i) + \mathrm{sat}(v_i^e)) \in \mathbb{L}_\infty$, $i \in \mathcal{V}$ given in Definition 1. In addition, by considering Definition 1 and (42), it further follows that $\mathrm{d}(\mathrm{sat}(s_i(t)) + \mathrm{sat}(v_i^e(t)))/\mathrm{d}t \in \mathbb{L}_\infty$, $i \in \mathcal{V}$. Thus, according to the Barbalat lemma [47], it can be concluded that $\lim_{t\to\infty}(\mathrm{sat}(s_i(t)) + \mathrm{sat}(v_i^e(t))) = 0$, $i \in \mathcal{V}$. Due to the strictly increasing property of $\mathrm{sat}(\cdot)$, we know that $\lim_{t\to\infty}(s_i(t) + v_i^e(t)) = 0$, $i \in \mathcal{V}$.

Next, let $\varrho_i = s_i + v_i^e$, $i \in \mathcal{V}$. It follows from (21) that:

$$v_i^e = \dot{p}_i^e = -\frac{1}{2} \sum_{j \in \mathcal{N}_i} a_{ij}\left(p_i^e - p_j^e\right) + \frac{\varrho_i}{2}, \quad i \in \mathcal{V}. \tag{50}$$

According to [48], the fact that $\lim_{t\to\infty} \varrho_i(t) = 0$, $i \in \mathcal{V}$ is sufficient to guarantee that $\lim_{t\to\infty}(p_i^e(t) - p_j^e(t)) = 0$, $i, j \in \mathcal{V}$ given in Assumption 2. It thus follows that $\lim_{t\to\infty} v_i^e(t) = 0$ and further that $\lim_{t\to\infty} s_i(t) = 0$, $i \in \mathcal{V}$.

Since the claimed two prerequisites are satisfied, it follows that the closed-loop position error system (41) is asymptotically stable, that is, $\lim_{t\to\infty} s_i(t) = 0$ and $\lim_{t\to\infty} v_i^e(t) = 0$, $i \in \mathcal{V}$. By considering (21), this implies that $\lim_{t\to\infty}(p_i^e(t) - p_j^e(t)) = 0$, $i, j \in \mathcal{V}$ given in Assumption 2. ∎

Remark 6: In contrast to the attitude loop where the convergence analysis of each attitude and estimation error $\tilde{\rho}_i$ is carried out simultaneously (i.e., Proposition 1), the convergence analysis of each estimation error $\tilde{m}_i$ is undertaken independently (i.e., Proposition 2) in the position loop by introducing the I&I adaption (24) for updating each mass estimation $\hat{m}_i$. Such an adaption manner can not only guarantee the accurate mass estimation but also effectively avoid potential invalidity of some operations [such as (45) and (47)] in the position consensus analysis arising from asymmetry when introducing heterogeneous masses.

In terms of Propositions 1 and 3, we finally introduce a theorem to sum up the overall stability result.

Theorem 1: Consider the ith VTOL UAV system (6)–(9). Suppose that Assumptions 1 and 2 hold. Given $\mathrm{tr}(I_3 - R_i^e(0)) \neq 4$, the proposed commanded force (23) and applied thrust (26) with adaptive laws (24) and (27) guarantee that the coordinated formation of a team of VTOL UAVs is achieved in the sense of (10).

Proof: Since Propositions 1 and 3 have shown that (20) is satisfied, according to Lemma 4, the concerned coordinated formation objective (10) is achieved. ∎

V. Simulations

A. Scenario I: Effectiveness Verification

In this section, a flight scenario is simulated to verify the effectiveness of the proposed distributed control algorithm. Suppose that there is a team of four quadrotors. The equation of motion of each individual complies with (6)–(9), while its applied thrust and torque are generated by rotating four equally spaced rotors. Intuitively

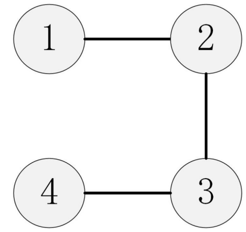

Fig. 1. Network topology $\mathcal{G}$.

TABLE I
Inertial Parameters

	Mass (kg)	Inertia matrix (kgm^2)
UAV 1	0.85	$\mathrm{diag}\{4.856, 4.856, 8.801\} * 10^{-2}$
UAV 2	1.2	$\mathrm{diag}\{1.522, 1.522, 3\} * 10^{-1}$
UAV 3	0.35	$\mathrm{diag}\{2.56, 2.56, 5.2\} * 10^{-2}$
UAV 4	3.4	$\mathrm{diag}\{3.54, 3.54, 6.54\} * 10^{-1}$

$$\begin{bmatrix} T_i \\ \tau_{i,x} \\ \tau_{i,y} \\ \tau_{i,z} \end{bmatrix} = \begin{bmatrix} 1 & 1 & 1 & 1 \\ 0 & -d_i & 0 & d_i \\ d_i & 0 & -d_i & 0 \\ C_i & -C_i & C_i & -C_i \end{bmatrix} \begin{bmatrix} f_{i,1} \\ f_{i,2} \\ f_{i,3} \\ f_{i,4} \end{bmatrix}, \quad i \in \mathcal{V} \tag{51}$$

where d_i is the distance from the quadrotor c.g. to the rotation axis of each rotor, C_i is the anti-torque coefficient, and $f_{i,j}$ ($j = 1, 2, 3, 4$) is the thrust generated by each rotor. It it trivial that each $f_{i,j}$ can be determined by the control thrust T_i and torque τ_i directly in terms of (51). Moreover, the network topology among quadrotors is depicted in Fig. 1. It can be examined that the connected condition claimed in Assumption 2 is satisfied. In addition, the inertial parameters of the quadrotors are given in Table I. Note that they are heterogeneous, where the maximum mass is almost ten times the minimum one. Four quadrotors are commanded to track a reference velocity $v_r(t) = [0.3\cos(2\pi t/23), 0.3\cos(4\pi t/23), 0.2]^T$ m/s while maintaining a prescribed formation pattern represented by

$$\Theta_x = \left[\theta_{ij,x}\right] = \begin{bmatrix} 0 & 0 & 4 & 4 \\ 0 & 0 & 4 & 4 \\ -4 & -4 & 0 & 0 \\ -4 & -4 & 0 & 0 \end{bmatrix} \mathrm{m}$$

$$\Theta_y = \left[\theta_{ij,y}\right] = \begin{bmatrix} 0 & 4 & 4 & 0 \\ -4 & 0 & 0 & -4 \\ -4 & 0 & 0 & -4 \\ 0 & 4 & 4 & 0 \end{bmatrix} \mathrm{m}$$

and $\Theta_z = [\theta_{ij,z}] = 0_{4\times 4}$. The initial positions are specified as $p_1(0) = [4, 4, -1]^T$ m, $p_2(0) = [3, -4, 1]^T$ m, $p_3(0) = [-5, -4, 2]^T$ m, and $p_4(0) = [-1, 3, -2]^T$ m with the initial velocities being 0, and the initial attitudes are chosen as $R_i(0) = I_3$, $i = 1, 2, 3, 4$ with the initial angular velocities being 0. The initial estimations are designated as $\hat{m}_1(0) = 1$ kg, $\hat{m}_2(0) = 4$ kg, $\hat{m}_3(0) = 1$ kg, $\hat{m}_4(0) = 4$ kg, and $\hat{J}_i(0) = 0.08 I_3$ kgm^2, $i = 1, 2, 3, 4$. The saturation function we choose is the hyperbolic tangent function $\tanh(\cdot)$.

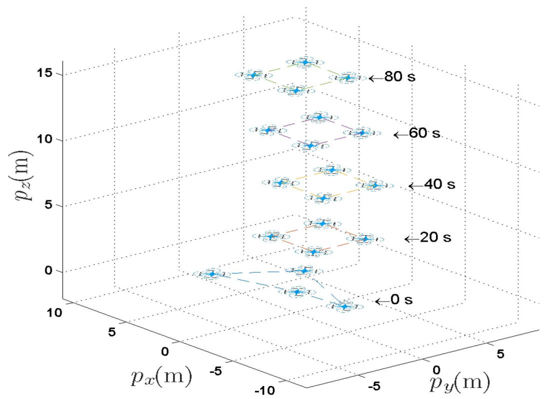

Fig. 2. Formation snapshot.

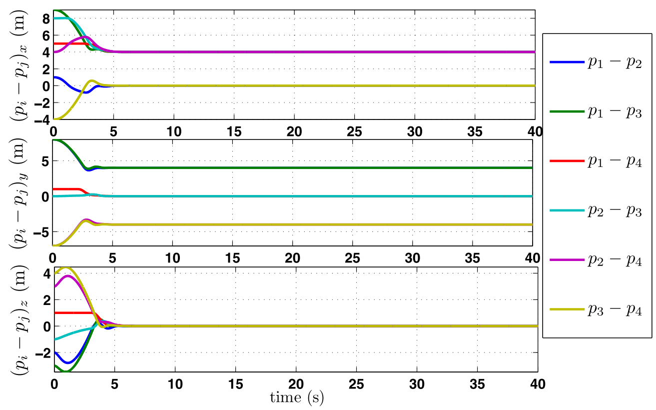

Fig. 3. Trajectories of position offsets.

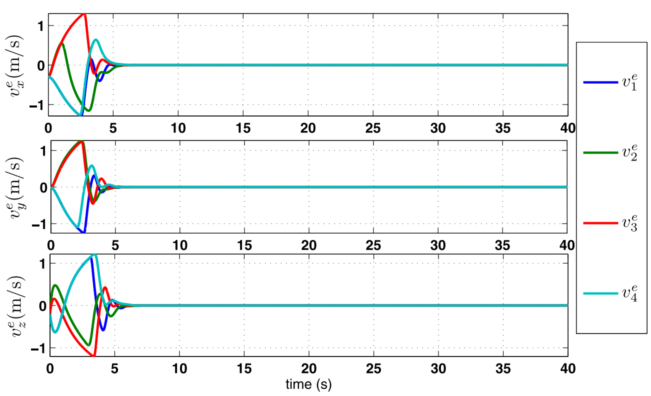

Fig. 4. Trajectories of velocity errors.

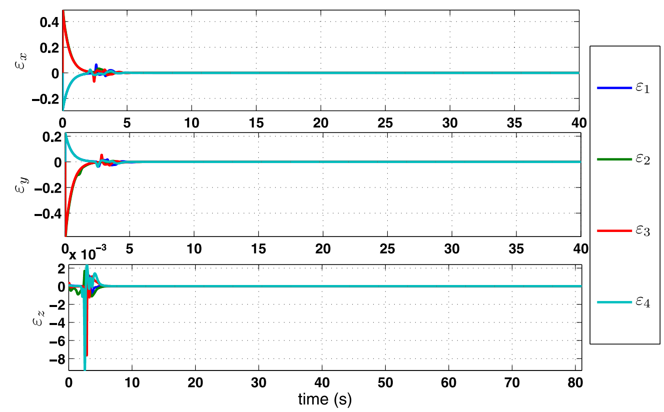

Fig. 5. Trajectories of attitude errors.

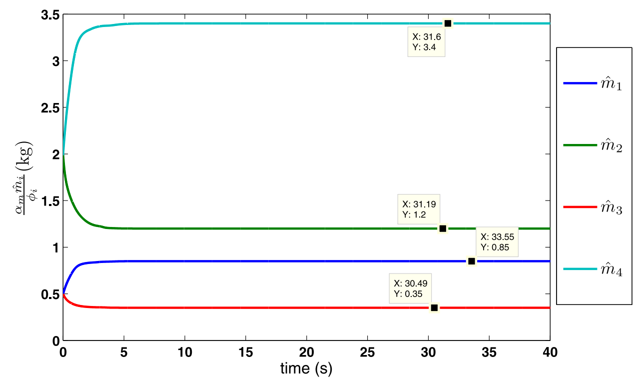

Fig. 6. Trajectories of mass estimations.

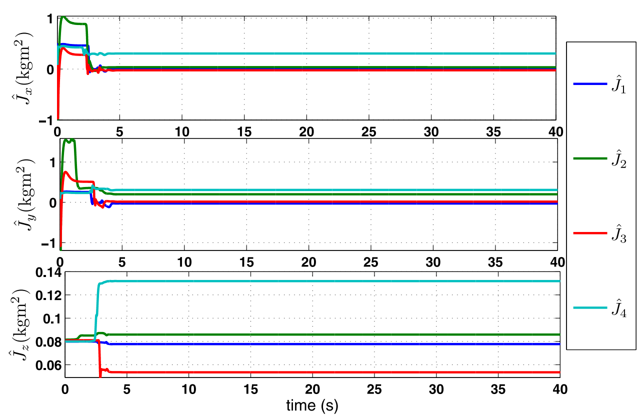

Fig. 7. Trajectories of inertia parameter estimations.

Moreover, by considering that the overall VTOL UAV system is under a hierarchical framework composed of an inner attitude loop and an outer position loop, it had better make the prior stability of the inner attitude loop in order for the stability of the outer position loop. Inspired by this fact, we specify attitude control parameters $\alpha_\varepsilon = 32$ and $\alpha_\omega = 32$ larger than the position control parameters $c_p = 4$, $\alpha_m = 1$, and $\alpha_p = 2$. In addition, the adaptive parameters are chosen as $c_\epsilon = 0.5$ and $\alpha_\rho = 10$. The simulation results are illustrated in Figs. 2–7.

Fig. 2 exhibits the formation evolution of the concerned VTOL UAVs. It can be observed that the prescribed pattern is formed within 20 s while being maintained afterward. Specifically, Fig. 3 shows that the position offsets between distinct UAVs asymptotically converge to their specified desired ones. Moreover, Figs. 4 and 5 show that the velocity and attitude errors driven by the proposed distributed control algorithm converge to origin asymptotically. In addition, Fig. 6 illustrates that the exponential convergence of the mass estimations to their actual values is guaranteed by the I&I adaption. Finally, it can be seen from Fig. 7 that the inertia parameter estimations are bounded.

B. Scenario II: Performance Comparison

To highlight the compensation performance of the proposed adaptive scheme, we next compare the proposed adaptive

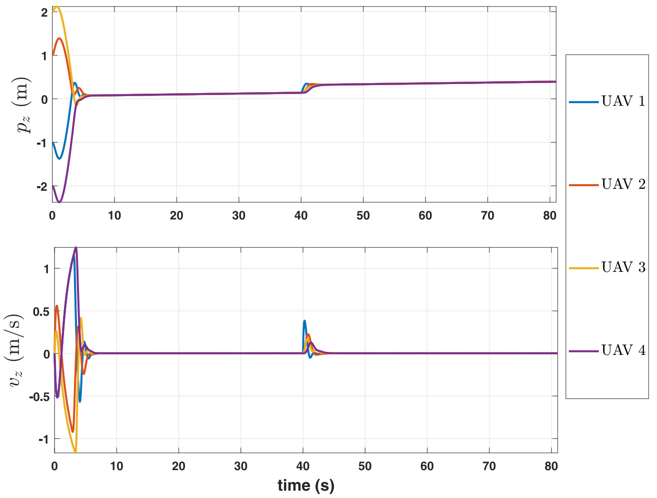

Fig. 8. Trajectories of position and velocity on the z_I-axis with proposed control.

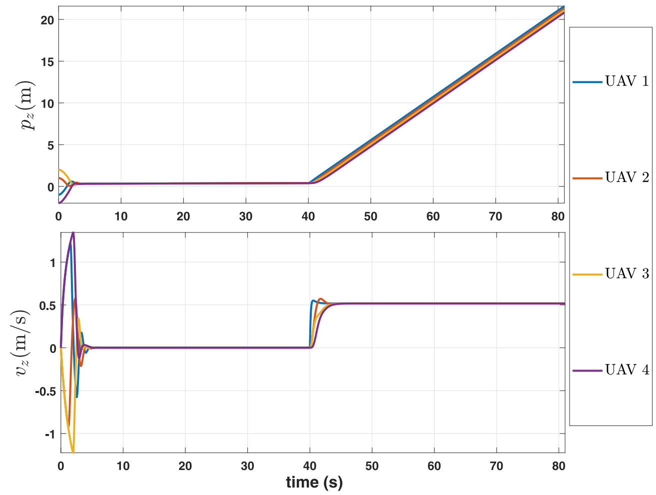

Fig. 9. Trajectories of position and velocity on the z_I-axis with control in [35].

distributed control algorithm with the one introduced in [35] without adaption. Suppose that the simulation setting here is the same as that of the previous scenario except that the third component of the reference velocity becomes 0. This means that all the VTOL UAVs are expected to complete the coordinated formation on some plane perpendicular to the z_I-axis. Moreover, suppose that there is a 30% mass drop at the first UAV at 40 s probably arising from a load toss. The comparison results are illustrated in Figs. 8 and 9. In particular, they exhibit the velocity tracking and position consensus results on the z_I-axis driven by two distributed control algorithms. By comparing the upper subfigures of these two figures, it can be observed that both two distributed control algorithms achieve the concerned formation objective until 40 s when the mass drop happens. After 40 s, the proposed distributed control algorithm with adaption still guarantees the collective motion on another plane perpendicular to the z_I-axis, whereas the collective motion driven by the distributed control algorithm in [35] diverges. To explain this phenomenon, we next compare the velocity tracking results in the lower subfigures of Figs. 8 and 9. It can be seen that the mass drop at 40 s brings in a velocity tracking error driven by the distributed control algorithm in [35], thereby leading to the position divergence. However, all the velocities driven by the proposed distributed algorithm come back to 0 with the help of the adaptive effect. By comparison, the proposed distributed adaptive control algorithm is of a better compensation performance than the one introduced in [35].

VI. Conclusion

An adaptive distributed control algorithm is developed in this article to achieve the coordinated formation control of heterogeneous VTOL UAVs in the presence of parametric uncertainties. The proposed control algorithm is in terms of a cascaded structure such that the position and attitude loops are surveyed in sequence. First, a distributed command force is synthesized for the position formation in the position loop, where an I&I adaption strategy is developed for the exponential mass estimation. Then, an applied thrust and a command attitude are extracted from the synthesized command force. Next, an applied torque with adaption is synthesized for the attitude tracking to the extracted command attitude in the attitude loop. It is proven in terms of the Lyapunov theory that the proposed distributed control algorithm guarantees the accomplishment of the concerned coordinated control objective of multiple VTOL UAVs via local information exchange. Finally, simulations are undertaken to confirm the effectiveness of the proposed control algorithm.

Appendix
Expressions of ω_i^c and $\dot{\omega}_i^c$

First, the command rotation matrix R_i^c extracted in (14) can be expressed in another form

$$R_i^c = \begin{bmatrix} R_{i,3} + \frac{R_{i,2}^2}{1+R_{i,3}} & -\frac{R_{i,1}R_{i,2}}{1+R_{i,3}} & R_{i,1} \\ -\frac{R_{i,1}R_{i,2}}{1+R_{i,3}} & R_{i,3} + \frac{R_{i,1}^2}{1+R_{i,3}} & R_{i,2} \\ -R_{i,1} & -R_{i,2} & R_{i,3} \end{bmatrix}.$$

According to [44], the command angular velocity ω_i^c is expressed by $\omega_i^c = [\sigma_{i,z}, \varsigma_{i,x}, -\sigma_{i,x}]^T$, where

$$\sigma_i = \begin{bmatrix} \sigma_{i,x} \\ \sigma_{i,y} \\ \sigma_{i,z} \end{bmatrix} = \frac{1}{\|u_i\|}\left(R_i^c\right)^T \Theta_i \Lambda_i \dot{u}_i$$

$$\varsigma_i = \begin{bmatrix} \varsigma_{i,x} \\ \varsigma_{i,y} \\ \varsigma_{i,z} \end{bmatrix} = \frac{1}{\|u_i\|}\Pi\left(R_i^c\right)^T \dot{u}_i$$

$$\Theta_i = \begin{bmatrix} -\frac{R_{i,2}}{1+R_{i,3}} & -\frac{R_{i,1}}{1+R_{i,3}} & \frac{R_{i,1}R_{i,2}}{(1+R_{i,3})^2} \\ \frac{2R_{i,1}}{1+R_{i,3}} & 0 & 1-\frac{R_{i,1}^2}{(1+R_{i,3})^2} \\ 0 & -1 & 0 \end{bmatrix}$$

$$\Pi = I_3 - \hat{e}_3\hat{e}_3^T, \quad \Lambda_i = R_i^c \Pi \left(R_i^c\right)^T.$$

In addition, the derivative of ω_i^c is expressed by $\dot{\omega}_i^c = [\phi_{i,z}, \varphi_{i,x}, -\phi_{i,x}]^T$, where

$$\phi_i = \begin{bmatrix} \phi_{i,x} \\ \phi_{i,y} \\ \phi_{i,z} \end{bmatrix} = \frac{1}{\|u_i\|}\Bigg[\Big(\big(\dot{R}_i^c\big)^T\Theta_i + \big(R_i^c\big)^T\dot{\Theta}_i\Big)\Lambda_i\dot{u}_i + \big(R_i^c\big)^T\Theta_i\Lambda_i\left(\ddot{u}_i - \frac{u_i^T\dot{u}_i}{\|u_i\|^2}\dot{u}_i\right)\Bigg]$$

$$\varphi_i = \begin{bmatrix} \varphi_{i,x} \\ \varphi_{i,y} \\ \varphi_{i,z} \end{bmatrix} = \frac{1}{\|u_i\|}\Pi\left[\big(\dot{R}_i^c\big)^T\dot{u}_i + \big(R_i^c\big)^T\left(\ddot{u}_i - \frac{u_i^T\dot{u}_i}{\|u_i\|^2}\dot{u}_i\right)\right]$$

$$\big(\dot{R}_i^c\big)^T = -\big(\omega_i^c\big)^\times\big(R_i^c\big)^T.$$

References

[1] L. Li, Z. Chen, Y. Wang, X. Zhang, N. Wang, "Robust task-space tracking for free-floating space manipulators by cerebellar model articulation controller," *Assembly Autom.*, vol. 39, no. 1, pp. 26–33, 2019.

[2] X. Yu, W. He, Y. Li, C. Xue, Y. Sun, and Y. Wang, "Adaptive NN impedance control for an SEA-driven robot," *Sci. China Inf. Sci.*, vol. 63, no. 5, 2020, Art. no. 159207.

[3] Y. Ren, M. Chen, and J. Liu, "Bilateral coordinate boundary adaptive control for a helicopter lifting system with backlash-like hysteresis," *Sci. China Inf. Sci.*, vol. 63, no. 1, 2020, Art. no. 119203.

[4] M. Hua, T. Hamel, P. Morin, and C. Samson, "Introduction to feedback control of underactuated VTOLvehicles: A review of basic control design ideas and principles," *IEEE Control Syst. Mag.*, vol. 33, no. 1, pp. 61–75, Feb. 2013.

[5] F. Giulietti, L. Pollini, and M. Innocenti, "Autonomous formation flight," *IEEE Control Syst. Mag.*, vol. 20, no. 6, pp. 34–44, Dec. 2000.

[6] L. Wang and H. Jia, "The trajectory tracking problem of quadrotor UAV: Global stability analysis and control design based on the cascade theory," *Asian J. Control*, vol. 16, no. 2, pp. 574–588, 2014.

[7] D. Invernizzi and M. Lovera, "Trajectory tracking control of thrust-vectoring UAVs," *Automatica*, vol. 95, pp. 180–186, Sep. 2018.

[8] M. Hua, T. Hamel, P. Morina, and C. Samson, "Control of VTOL vehicles with thrust-tilting augmentation," *Automatica*, vol. 52, pp. 1–7, Feb. 2015.

[9] B. Tian, L. Liu, H. Lu, Z. Zuo, Q. Zong, and Y. Zhang, "Multivariable finite time attitude control for quadrotor UAV: Theory and experimentation," *IEEE Trans. Ind. Electron.*, vol. 65, no. 3, pp. 2567–2577, Mar. 2018.

[10] N. Cao and A. F. Lynch, "Inner–outer loop control for quadrotor UAVs with input and state constraints," *IEEE Trans. Control Syst. Technol.*, vol. 24, no. 5, pp. 1797–1804, Sep. 2016.

[11] Y. Zou, "Trajectory tracking controller for quadrotors without velocity and angular velocity measurements," *IET Control Theory Appl.*, vol. 11, no. 1, pp. 101–109, Jan. 2017.

[12] A. Astolfi and R. Ortega, "Immersion and invariance: A new tool for stabilization and adaptive control of nonlinear systems," *IEEE Trans. Autom. Control*, vol. 48, no. 4, pp. 590–606, Apr. 2003.

[13] J. Hu and H. Zhang, "Immersion and invariance based command-fitered adaptive backstepping control of VTOL vehicles," *Automatica*, vol. 49, no. 7, pp. 2160–2167, 2013.

[14] A. Roberts and A. Tayebi, "Adaptive position tracking of VTOL UAVs," *IEEE Trans. Robot.*, vol. 27, no. 1, pp. 129–142, Feb. 2011.

[15] B. Zhao, B. Xian, Y. Zhang, and X. Zhang, "Nonlinear robust sliding mode control of a quadrotor unmanned aerial vehicle based on immerison and invariance method," *Int. J. Robust Nonlin. Control*, vol. 25, no. 18, pp. 3714–3731, 2014.

[16] B. Zhao, B. Xian, Y. Zhang, and X. Zhang, "Nonlinear robust adaptive tracking control a quadrotor UAV via immersion and invariance methodology," *IEEE Trans. Ind. Electron.*, vol. 62, no. 5, pp. 2891–2902, May 2015.

[17] B. Yun, B. Chen, K. Y. Lum, and T. H. Lee, "Design and implementation of a leader–follower cooperative control system for unmanned helicopters," *J. Control Theory Technol.*, vol. 8, no. 1, pp. 61–68, 2010.

[18] D. A. Mercado, R. Castro, and R. Lozano, "Quadrotors flight formation control using a leader–follower," in *Proc. Eur. Control Conf.*, Zürich, Switzerland, 2013, pp. 3858–3863.

[19] K. D. Do, "Coordnation control of quadrotor VTOL aircraft in three-dimensional space," *Int. J. Control*, vol. 88, no. 3, pp. 543–558, 2015.

[20] A. Kushleyev, D. Melliger, and V. Kumar, "Towards a swarm of agile micro quadrotors," in *Proc. Robot. Sci. Syst. Conf.*, Sydney, NSW, Australia, 2012, pp. 287–300.

[21] F. Liao, R. Teo, J. Wang, X. Dong, F. Lin, and K. Peng, "Distributed formation and reconfiguration control of VTOL UAVs," *IEEE Trans. Control Syst. Technol.*, vol. 25, no. 1, pp. 270–277, Jan. 2017.

[22] W. Ren, "On consensus algorithms for double-integrator dynamics," *IEEE Trans. Autom. Control*, vol. 53, no. 6, pp. 1503–1509, Jul. 2008.

[23] W. Ren and R. W. Beard, "Consensus seeking in multiagent systems under dynamically changing interaction topologies," *IEEE Trans. Autom. Control*, vol. 50, no. 5, pp. 655–661, May 2005.

[24] Y. Zhang, J. Sun, H. Liang, and H. Li, "Event-triggered adaptive tracking control for multi-agent systems with unknown disturbances," *IEEE Trans. Cybern.*, vol. 50, no. 3, pp. 890–901, Mar. 2020, doi: 10.1109/TCYB.2018.2869084.

[25] Z. Chen, Q. Han, Y. Yan, and Z. Wu, "How often should one update control and estimation: review of networked triggering techniques," *Sci. China Inf. Sci.*, vol. 63, no. 5, 2020, Art. no. 150201.

[26] D. Li, W. Zhang, W. He, C. Li, and S. Ge, "Two-layer distributed formation-containment control of multiple Euler–Lagrange systems by output feedback," *IEEE Trans. Cybern.*, vol. 49, no. 2, pp. 675–687, Feb. 2019.

[27] A. Abdessameud and A. Tayebi, "Formation control of VTOL UAVs," in *Proc. 48th IEEE Conf. Decis. Control*, Shanghai, China, 2009, pp. 3454–3459

[28] A. Abdessameud and A. Tayebi, "Formation control of VTOL UAVs without linear-velocity measurements," in *Proc. Amer. Control Conf.*, 2010, pp. 2107–2112.

[29] A. Abdessameud, I. G. Polushin, and A. Tayebi, "Motion coordination of thrust-propelled underactuated vehicles with intermittent and delayed communications," *Syst. Control Lett.*, vol. 79, pp. 15–22, May 2015.

[30] H. Du, W. Zhu, G. Wen, Z. Duan, and J. Lü, "Distributed formation control of multiple quadrotor aircraft based on nonsmooth consensus algorithms," *IEEE Trans. Cybern.*, vol. 49, no. 1, pp. 342–353, Jan. 2019.

[31] Y. Zou and Z. Meng, "Distributed hierarchical control for multiple vertical takeoff and landing UAVs with a distance-based network topology," *Int. J. Robust Nonlin. Control*, vol. 29, no. 9, pp. 2573–2588, 2019.

[32] Y. Zou and Z. Meng, "Coordinated trajectory tracking of multiple vertical take-off and landing UAVs," *Automatica*, vol. 99, pp. 33–40, Jan. 2019.

[33] X. Dong, Y. Zhou, Z. Ren, and Y. Zhong, "Time-varying formation control for unmanned aerial vehicles with switching interation topologies," *Control Eng. Practice*, vol. 46, pp. 26–36, Jan. 2016.

[34] X. Dong, Y. Zhou, Z. Ren, and Y. Zhong, "Time-varying formation tracking for second-order multi-agent systems subjected to switching topologies with application to quadrotor formation flying," *IEEE Trans. Ind. Electron.*, vol. 64, no. 6, pp. 5014–5024, Jun. 2017.

[35] Y. Zou, Z. Zhou, X. Dong, and Z. Meng, "Distributed formation control for multiple vertical takeoff and landing UAVs with switching topologies," *IEEE/ASME Trans. Mechatronics*, vol. 23, no. 4, pp. 1750–1761, Aug. 2018.

[36] Y. Zhang, Z. Deng, and Y. Hong, "Distributed optimal coordination for multiple heterogeneous Euler–Lagrangian systems," *Automatica*, vol. 79, pp. 207–213, May 2017.

[37] J. Mei, W. Ren, J. Chen, and G. Ma, "Distributed adaptive coordination for multiple Lagrangian systems under a directed graph without using neighbors' velocity information," *Automatica*, vol. 49, no. 6, pp. 1723–1731, 2013.

[38] J. Mei, W. Ren, and J. Chen, "Distributed consensus of second-order multi-agent systems with heterogeneous unknown inertias and control gains under a directed graph," *IEEE Trans. Autom. Control*, vol. 61, no. 8, pp. 2019–2034, Aug. 2016.

[39] S. Chen, D. W. C. Ho, L. Li, and M. Liu, "Fault-tolerant consensus of multi-agent system with distributed adaptive protocol," *IEEE Trans. Cybern.*, vol. 45, no. 10, pp. 2142–2155, Oct. 2015.

[40] A. R. Mehrabian and K. Khorasani, "Constrained distributed cooperative synchronization and reconfigurable control of heterogeneous networked Euler–Lagrange multi-agent systems," *Inf. Sci.*, vol. 370–371, pp. 578–597, Nov. 2016.

[41] M. Shuster, "A survey of attitude representations," *J. Astronautical Sci.*, vol. 41, no. 4, pp. 439–517, 1993.

[42] A. Abdessameud and A. Tayebi, *Motion Coordinated for VTOL Unmanned Aerial Vehicles*. London, U.K.: Springer, 2013.

[43] Y. Zou and Z. Zheng, "A robust adaptive RBFNN augmenting backstepping control approach for a model-scaled helicopter," *IEEE Trans. Control Syst. Technol.*, vol. 23, no. 6, pp. 2344–2352, Nov. 2015.

[44] Y. Zou, "Nonlinear hierarchical control for quad-rotors with rotation matrix," *Int. J. Control*, vol. 90, no. 7, pp. 1308–1318, 2017.
[45] Y. Zhao, Y. Liu, G. Wen, and G. Chen, "Distributed optimization for linear multiagent systems: Edge- and node-based adaptive designs," *IEEE Trans. Autom. Control*, vol. 62, no. 7, pp. 3602–3609, Jul. 2017.
[46] A. Levant, "Higher-order sliding modes, differentiation and output feedback control," *Int. J. Control*, vol. 76, nos. 9–10, pp. 924–941, 2003.
[47] H. Khalil, *Nonlinear Systems*, 3rd ed. Englewood Cliffs, NJ, USA: Prentice-Hall, 2002.
[48] G. Shi and K. H. Johansson, "Robust consensus for continuous-time multiagent dynamics," *SIAM J. Control Optim.*, vol. 51, no. 5, pp. 3673–3691, 2013.

Yao Zou received the B.S. degree in automation from the Dalian University of Technology, Dalian, China, in 2010, and the Ph.D. degree in control science and engineering from Beihang University (BUAA, formerly named Beijing University of Aeronautics and Astronautics) Beijing, China, in 2016.

He was a Postdoctoral Research Fellow with the Department of Precision Instrument, Tsinghua University, Beijing, from 2017 to 2018. He is currently an Associate Professor with the School of Automation and Electrical Engineering, University of Science and Technology Beijing, Beijing. His current research interests include nonlinear control, unmanned aerial vehicle control, and multiagent control.

Haojie Zhang received the B.Sc. degree from Central South University, Changsha, China, in 2008, and the Ph.D. degree from the Beijing Institute of Technology, Beijing, China, in 2013.

He is currently an Associate Professor with the School of Automation and Electrical Engineering, University of Science and Technology Beijing, Beijing. His main research interests include intelligent decision and planning and control for mobile robots.

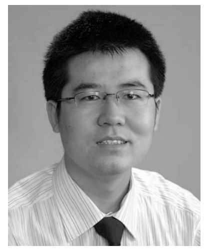

Wei He (Senior Member, IEEE) received the B.Eng. and M.Eng. degrees from the College of Automation Science and Engineering, South China University of Technology, Guangzhou, China, in 2006 and 2008, respectively, and the Ph.D. degree from the Department of Electrical and Computer Engineering, National University of Singapore, Singapore, in 2011.

He is currently working as a Full Professor with the School of Automation and Electrical Engineering, University of Science and Technology Beijing, Beijing, China. He has coauthored three books published in Springer and published over 100 international journal and conference papers. His current research interests include robotics, distributed parameter systems, and intelligent control systems.

Prof. He was awarded a Newton Advanced Fellowship from the Royal Society, U.K., in 2017. He was a recipient of the IEEE SMC Society Andrew P. Sage Best Transactions Paper Award in 2017. He is serving as the Chair of the IEEE SMC Society Beijing Capital Region Chapter. Since 2018, he has been the Chair of Technical Committee on Autonomous Bionic Robotic Aircraft, IEEE Systems, Man and Cybernetics Society. He is serving as an Associate Editor for the IEEE TRANSACTIONS ON ROBOTICS, the IEEE TRANSACTIONS ON NEURAL NETWORKS AND LEARNING SYSTEMS, the IEEE TRANSACTIONS ON CONTROL SYSTEMS TECHNOLOGY, the IEEE TRANSACTIONS ON SYSTEMS, MAN, AND CYBERNETICS: SYSTEMS, *SCIENCE CHINA Information Sciences*, the IEEE/CAA JOURNAL OF AUTOMATICA SINICA, and *Neurocomputing*, and an Editor for the *Journal of Intelligent & Robotic Systems*. He is the member of IEEE CSS Conference Editorial Board.